Dynamic Neural Network Model for Environmental Monitoring of Vehicle Pollution in Urban Streets

Vladimir Shepelev
Ph.D.
Department of Automobile Transportation,
South Ural State University
Russia

Aleksandr Glushkov
Ph.D.
Department of Mathematical and
Computer Modeling
South Ural State University
Russia

Olga Ivanova
Ph.D.
Computer Science Department
South Ural State University
Russia

Ksenia Bastrykina
Computer Science Department
South Ural State University
Russia

The gas pollution of the air by vehicle emissions in a sustainable, smart city is an undeniable and urgent problem that requires new methods of solution. In order to take administrative measures to improve air quality, it is necessary to have a reliable tool for instant assessment of current air pollution at road intersections as places of the largest accumulation of vehicles. This article describes a mathematical model and its software implementation based on neural network technology, which allows continuous monitoring of emissions of nine types of pollutants from various categories of standing and moving vehicles with such parameters as speed, coordinates, and idle time. Authors developed a dataset for the dynamic neural network training, which consists of 60,000 labeled images. The model calculates the pollution level of an air basin in an area determined by the visibility zone of an outdoor video surveillance camera and a height of 2 meters. Unlike existing models, the proposed solution works in real time mode, can be embedded into the existing infrastructure for monitoring road intersections, and takes into account current weather conditions: wind strength and direction. This allowed the authors to verify the results of calculations with instrumental measurements of a mobile environmental laboratory, to achieve high accuracy in detecting current air pollution for further management of environmental risks associated with road traffic.

Keywords: *traffic flows; pollutant emissions; concentration of emissions; area sources of emissions; neural network model; software system.*

1. INTRODUCTION

Numerous studies have established that hazardous sub–stances entering the air from the exhaust gases of vehicles cause irreparable harm to the health of urban populations [1-4]. Intersections which are characterized by congestion and sharp changes in the traffic patterns of numerous vehicles, are especially unfavourable situations [5-8]. An adequate assessment of the current level of emissions and their distribution at intersections is therefore of vital importance [9].

Changes in traffic patterns within a signal-controlled intersection and frequent changes in wind direction increase the dispersion of harmful emissions in street canyons [10]. Sharp accelerations over short distances at intersections give peak emission values [11-13].

The authors in [14, 15] examined the content of particulate matter (PM1, PM2.5, and PM10) in the air depending on the configuration of intersections, show–ing that a traffic circle can reduce the concentration of PM10 by up to 50% compared to a three-turn inter–section. Cerdeira et al. [16] studied the dispersion of harmful emissions depending on the type of intersection (traffic circles and signal-controlled intersections) using the ADMS-urban model to obtain a spatial emission dispersion model. The model used traffic parameters (vehicle speed, fuel type, time of the day, city street canyon, etc.) and meteorological parameters (wind spe–ed and direction, humidity, air temperature, etc.). The modelling revealed that winter is less favourable for the dispersion of emissions, and traffic circles have an environmental advantage compared to signal-controlled intersections.

The authors in [17], refined and improved the CAL3QHC model taking into account vehicle dece–leration and acceleration at a signal-controlled inter–section and proposed two schemes for reducing vehicle emissions: Green light optimal speed advisory (GLOSA) and the structure of an obstacle-free access road, which can reduce pollution levels by 20–22%.

A study of the diffusion of harmful traffic-related emissions showed that different building heights in a street canyon and wind speed affect the dispersion of harmful emissions. The diffusion coefficient and the stabilization degree of harmful emissions during the day also differ depending on sunlight [18]. Dense urban development significantly reduces wind speed, which leads to the accumulation of harmful traffic-related emissions, especially at intersections [19].

The dispersion of emissions is associated with many factors, such as wind speed and road geometry. In [6], the authors developed three dispersion models and presented a GIS platform visualizing the concentration of harmful emissions at the observed point.

Received: September 2024, Accepted: December 2024
Correspondence to: Vladimir Shepelev, Department of Automobile Transportation, South Ural State University
Lenin prospekt 76, 454080 Chelyabinsk, Russia
E-mail: shepelevvd@susu.ru
doi: 10.5937/fme2501051S

Air-pollution monitoring quantifies the concentration of one or several substances but does not identify the cause of pollution [20]. Such modelling can help describe and forecast the dispersion of harmful emissions and develop appropriate measures to reduce the negative impact [21, 22].

Chauhan et al. [23] used VISSIM's add on EnViVer module to simulate the assessment of vehicle-related emissions at an urban intersection depending on the characteristics of the intersection, the vehicle types, and the time interval of green traffic light signals.

Pospisil and Jicha [24] developed a dispersion model based on the Eulerian-Lagrangian approach to moving objects to reduce the negative impact of transport emissions in urban canyons. The model describes the concentration fields of air pollution under different traffic-light operating modes and traffic dynamics in an urban canyon. Pepe et al. [25] also used a Lagrangian dispersion model (AUSTAL2000) to model local air quality within a city. However, air quality can be assessed more accurately using a hybrid modelling system which synthesizes chemical and transport models.

To predict PM10 concentration at a busy urban intersection, the authors in [26] developed a semi-empirical box model based on instantaneous speed and acceleration. To predict hourly average concentrations of O3 and NOx, Sekar et al. [27] used an artificial neural network with meteorological data, traffic data, and transport emissions as inputs.

The accuracy of modelling depends on the input data, such as vehicle behaviour. To assess the impact of road traffic on emissions and air quality, Fallah Shorshani et al. [28] considered two approaches: the behaviour of individual and groups of vehicles through the network. The latter approach showed more accurate emissions indicators, which provides for a better assessment of air quality.

During modelling, vehicle-related emission factors are typically calculated based on the measurements of individual vehicles. Lejri et al. [29] analysed the sensitivity of two models–PHEM (Passenger Car and Heavy-Duty Emission Model) and COPERT (Computer Program to Calculate Emissions from Road Transport) – to traffic dynamics at the scale of a road segment. PHEM more effectively calculates emissions along the vehicle's trajectory, but the calculation inaccuracy is explained by the lack of a real composition of vehicles by types. In the COPERT model, the use of average speed data also introduces a significant error into the emissions calculation.

Sun et al. [17] studied the performance of three dispersion models at signal-controlled intersections: CAL3QHC (California Line Source Model with Queuing and Hot Spot Calculations), ENVI-met, and Fluent for PM2.5, taking into account the height of the street canyon. The ENVI-met and CAL3QHC models use time-averaged idle emission factors. The ANSYS Fluent software was used to simulate air flows and turbulence at an intersection to obtain the dispersion of pollutants in a street canyon. Fluent showed better results in predicting PM2.5 concentrations, while ENVI-met is better at assessing correlations between PM concentrations and meteorological factors.

Zheng and Yang [30] also compared harmful emission dispersion models taking into account the turbulence created by the traffic flow itself.

Neural networks and soft computing techniques can determine the air concentrations of various substances given the stochastic nature of input data, such as wind speed, traffic intensity, and weather conditions. To determine the CO2 concentration, the authors [31] compare several computational methods, such as a feed–forward neural network, a recurrent neural network, and a hybrid neuro-fuzzy estimator of CO2 emission levels.

Traffic systems have recently been subject to widespread video surveillance systems and have become more intelligent [32]. Visual representations of traffic data in a management system are essential in energy conservation and reducing traffic congestion and emissions [33]. The results once again proved the potential of artificial intelligence in assessing such complex processes as the dispersion of harmful emissions.

Our research is focused on the development of a software system that provides for the real-time evaluation of the distribution of harmful emissions at intersections based on traffic intensity and meteorological conditions.

2. A CONCEPTUAL MODEL FOR CALCULATING THE POLLUTANT CLOUD CONCENTRATION AT AN INTERSECTION

The main requirement for a general computational model of a pollutant cloud concentration for an intersection is to determine the pollutant concentration for each point in the cloud in real time, at an acceptable update frequency. It is advisable to divide the cloud concentration for a specific intersection, which has been predetermined in constant geometric dimensions, into several identical squares and to calculate the concentration of each pollutant from the entire traffic flow at the intersection in real time. The concentration of pollutants is considered constant within one square. Specific numerical values of the parameters of the conceptual model (the grid of squares of the concentration cloud, intersection area, calculation update time, etc.) are shown when considering the software calculation system.

The conceptual model for calculating pollutant concentrations for an intersection is shown in Fig. 1, which shows a grid of squares of the pollutant dispersion cloud with the calculation of their concentration and the intersection, which is the source of pollutants from all vehicles located there. The conceptual model is based on the capabilities of "AIMS eco" a real-time monitoring of vehicle-related pollutant emissions system [34] previously created by the authors. This system is built using a neural network and analyses in real time a video stream of vehicles at an intersection recording the number of vehicles, their types, average speed, time spent at the intersection, etc. Based on these parameters, the system determines the intensity of traffic flows every 20 minutes and the level of emissions of the main pollutants at the intersection every hour.

The frequency of updating information on pollutant concentrations in the dispersion cloud is assumed to be

from 5 to 20 seconds. This assumption determines our approach of dividing the entire intersection area into a reasonable set of area sources that differ significantly in the number of vehicles and, accordingly, in the rate of pollutant emissions per time interval tk.

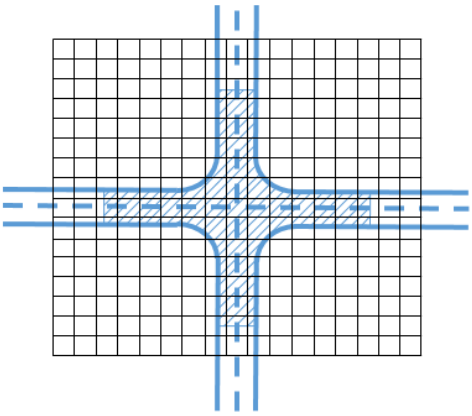

Figure 1. A grid of the pollutant cloud concentration and the intersection

According to the [35], the ground level concen–tration of pollutants at a fixed point in an area if there is a group of emission sources is determined by equation (1) as the sum of the concentrations of this pollutant from individual emission sources at a given wind direction and speed:

$$C=C_1+C_2+\ldots+C_N, \quad (1)$$

where C_1, C_2, ..., C_N are the concentrations of pollutants from the first, second, ..., N-th emission sources, respectively, located on the windward side.

Individual sources of pollutant emissions are all ve–hicles passing through the intersection at a given time.

According to the [35], in order to simplify calcu–lations, the number of such linear emission sources can be reduced by combining them into auxiliary emission sources, which are introduced to calculate the dispersion of pollutants from the entire intersection area. There–fore, let us imagine the entire area of the intersection as a set N of small area sources C_{Si}, (i=[1, N]), each of which includes all the vehicles located in this area in the time interval. Then equation (1) for each m-th grid square Cm of the pollutant concentration cloud is:

$$C(x_m, y_m)=\sum_{i=1}^{N} C_S(x_m-\zeta_i, y_m-\eta_i), \quad (2)$$

where (x_m, y_m) is the center point of the m-th grid square of the pollutant concentration cloud; (ξ_i,η_i) is the center point of the i-th area source $S(\xi_i,\eta_i)$ of the pollutant at the intersection.

Fig. 2 shows such the calculation algorithm as the sum of the concentrations in any grid square of the pollutant concentration cloud from several area sources C_{Si} (in the general case, from all sources).

The calculated pollutant concentration is not taken into account immediately in the cloud grid square, but only after the period during which the pollutants reach them. This time is calculated based on the distance from the center of the area emission source to the center of the grid square and the wind speed. The resulting concentrations are summed up, taking into account the time delay to reach each square of the cloud grid.

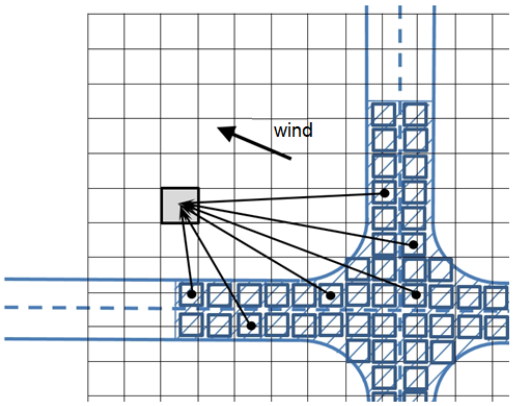

Figure 2. The sum of pollutant concentrations in a grid square from several area emission sources

The calculation model should take into account the time interval t_k of calculating pollutant emissions from multiple area sources of the intersection for updating information on pollutant concentrations in the grid squares of the concentration cloud. This corresponds to the calculation of pollutant emissions in the i-th area $S(\xi_i,\eta_i)$ from all vehicles located there during the time interval t_k. Equation (2) is transformed into:

$$C^{t_k}(x_m, y_m)=\sum_{i=1}^{N} C_S^{t_k}(x_m-\zeta_i, y_m-\eta_i), \quad (3)$$

which reflects the general algorithm – updated with a frequency of t_k monitoring over m grid squares of the pollutant concentration dissipation cloud, from N area sources of pollutant emissions which make up the entire intersection.

2.1 A conceptual calculation model taking into account multiple area sources of pollutant emissions

Let us consider the logical modeling procedure for calculating the concentration of pollutants in the m-th square of the concentration dispersion grid when the roadway of an intersection is divided into many area sources. The reference calculation formulas of [35] are adjusted according to the conceptual model adopted in the work.

STEP 1. In the general case, the concentration C_s of pollutants from a source which is emitting pollutants into the atmospheric air from an intersection occupying a region S with an area S_I is calculated by:

$$C_S(x_m, y_m)=\frac{1}{S_I}\iint_S (x_m-\zeta_i, y_m-\eta_i)\,d\zeta\,d\eta, \quad (4)$$

where $C(x_m-\xi_i,\ y_m-\eta_i)$ is the pollutant concentration created at the reference point (x_m,y_m) by a point emission source located at point (ξ, η) in region S, and the integral in the formula is calculated for this region. Point emission sources in the area S_I of the intersection are single vehicles of different types.

STEP 2. Since the neural network in the AIMS eco system tracks the trajectory of each vehicle within the

intersection, in the calculations we replace the single area source of pollutants from the intersection with a set of linear sources corresponding to the trajectory of each vehicle when their movement falls within the reporting time. Thus, in the particular case of one linear emission source located on the underlying surface, the pollutant concentration C_l is calculated by equation (5):

$$C_l(x_m, y_m, z_m) = \frac{1}{|L|}\int_L (x_m - \zeta_i, y_m - \eta_i, z_m)dl, , \quad (5)$$

where $|L|$ is the length of the specified segment, and the integral is calculated along this segment; $C(x_m-\xi_i, y_m-\eta_i, z_m)$ is the pollutant concentration created at the reference point (x_m, y_m, z_m) by a point emission source located at point (ξ, η, z) of segment L. The underlying surface at a constant vertical level z_m is a ground layer with a height H of no more than 2 m, so we will omit the coordinate z_m.

STEP 3. The Order#804 [35] provides for the use of the modified equation (5) for one moving vehicle if a linear emission source approximates emissions from a point source (one vehicle) of rate $M(t)$, which, during the averaging time, moves at a positive speed $v(t)$ along segment L, the pollutant concentration C_l is calculated by:

$$C_l(x_m, y_m) = \int_L \frac{M(l)\cdot C'(x_m - \zeta_i, y_m - \eta_i)}{v(l)}dl, , \quad (6)$$

where $M(l)$ and $v(l)$ are $M(t)$ and $v(t)$ values corres–ponding to time t when the moving emission source is at point $l=(\xi, \eta)$; C' is the concentration at point (x_m, y_m,) from a single pollutant emission source of a unit rate located at point (ξ, η), which is calculated according to the formulas given in [35].

Equation (6) is supplemented by the sum for all vehicles K moving along trajectories L_k along the roadway of the entire intersection:

$$C_S(x_m, y_m) = \sum_{k=1}^{K}\left(\int_{L_k}\frac{M_k(l_k)\cdot}{v_k(l_k)}dl\right)\times \times C'(x_m - \zeta_i, y_m - \eta_i) \quad . \quad (7)$$

STEP 4. In the calculations, we rely on the disc–retization of the integral in equation (7). Thus, accor–ding to [35], if the calculation of emission dispersion does not provide for the automatic calculation of the integrals that appear in the formulas for the con–centration of pollutants from curvilinear, area, and volumetric sources, these sources can form the set of point sources for the calculation. This corresponds exactly to the real capabilities of a neural network, which determines pollutant emissions from each vehicle along its trajectory through an intersection.

We divide the set of linear emission sources corres–ponding to all vehicles moving through the intersection into N area sources, which determine the total pollutant emissions from vehicles located in a given area S_i in the current time interval t_k. In this case, the calculation of pollutant concentrations in the m-th square of the dissipation cloud grid in t_k is transformed into:

$$C^{t_k}(x_m, y_m) = \sum_{i=1}^{N}\left(\sum_{k=1}^{K}\left(\int_{L_k}\frac{M_k(l_k)\cdot}{v_k(l_k)}dl\right)\times \times C'(x_m - \zeta_i, y_m - \eta_i)\right). \quad (8)$$

Taking into account that the integral is calculated for t_k and in view of its possible discretization, we obtain the following equation for the total rate M_i^{tk} of pollutant emission from the i-th area source for all K vehicles moving during t_k along the i-th area source:

$$M_i^{t_k} = \sum_{k=1}^{K}\left(\int_{L_k}\frac{M_k(l_k)\cdot}{v_k(l_k)}dl\right) = \sum_{k=1}^{K}(M_{k_i}\cdot t_k). \quad (9)$$

The Eq. (8) is then transformed into the final form:

$$C^{t_k}(x_m, y_m) = \sum_{i=1}^{N}\left(M_i^{t_k}\cdot C_i'(x_m - \zeta_i, y_m - \eta_i)\right), \quad (10)$$

Here we generally take into account pollutant emi–ssions from all vehicles only fully present in S_i during t_k.

Two more mathematical models are needed to apply the calculation model according to Eq. (10) in practice:

- the calculation of the rate M_i^{tk} of pollutant emis–sions from all vehicles of different types, those standing at the red traffic light and those moving at an arbitrary average speed in Si during t_k;
- the calculation of the concentration C'_i at point (x_m, y_m,) from a single area pollutant emission source of a unit rate located at point (ξ_i, η_i).

3. A MODEL FOR CALCULATING THE RATE OF POLLUTANT EMISSIONS FROM AN AREA SOURCE

The total rate of pollutant emissions M_i^{tk} in area S_i of the i-th area source determined by equation (9) is defined as the total rate of emissions from all vehicles in area S_i during time t_k. The calculation should be adjus–ted for moving vehicles not in area S_i during time t_k and provide for adding a component that takes into account pollutant emissions from vehicles standing at the red traffic light.

The calculation of the two components of M^{tk} is regulated by [35]. The specific mileage emissions of various pollutants M_m are specified in g/km for moving vehicles, while specific pollutant rates M_s are specified directly in g/min for vehicles at red traffic lights.

The following equation is used to determine the mileage rates of pollutant emissions M_{MR} in grams over time t_k measured in seconds:

$$M_{MR} = \frac{1}{3600}\cdot r_V \cdot M_m \cdot V \cdot t_k, \quad (11)$$

where r_V is a standardized correction factor taking into account the average vehicle speed; M_m are the stan–dardized specific mileage emissions of various pol–lutants for vehicles of various groups (g/km); V is the average vehicle speed (km/h).

The equation to determine the total rate M_i^{tk} of pollution emissions (reduced to per second) for the i-th area source is determined on the interval of time t_k as

the sum of emissions for all standing (K_{si}) and all moving (K_{mi}) vehicles within area S_i:

$$M_i^{t_k} = \frac{1}{60} \cdot \sum_{j=1}^{K_{sj}} M_{sj} \cdot t_j^{idle} + \\ + \frac{1}{3600} \cdot \sum_{l=1}^{K_{mj}} r_{Vl} \cdot M_{ml} \cdot V_l \cdot t_{Vl}, \quad (12)$$

where t_j^{idle} is the real idle time of the j-th vehicle during time t_k; as a rule, $t_j^{idle} = t_k$; t_{Vl} is the real movement time of the l-th vehicle at the average speed Vl during time t_k within area S_i; in the general case, $t_{Vl} \leq t_k$.

Equation (11) is similarly used to calculate pollutant emission rates for all N area sources representing the intersection. The calculation can be based on the data from a neural convolutional network, which records the classificatory group of vehicles, their speeds, and the time spent in each of the N areas S_i.

4. AN ALGORITHMIC MODEL FOR CALCULATING CM CONCENTRATION AT AN ARBITRARY POINT FROM A SINGLE AREA POLLUTANT SOURCE

All the necessary mathematical equations for this algo–rithmic model are presented step-wise in the relevant chapters of the to the Order#804 [35] and given below with the adaptation corrections for the conceptual model.

Step 1. Calculation of the maximum ground level concentration C_m, dangerous wind speed U_m, and dis–tance X_m.

In the general case, the maximum ground level pol–lutant concentration C_m (mg/m^3), when pollutants are emitted from a single point source with a round orifice, is achieved at a dangerous wind speed U_m, at the dis–tance X_m from the emission source, and is determined as:

$$C_m = \frac{A \cdot M \cdot F \cdot m \cdot n \cdot \eta}{H^2 \cdot \sqrt[3]{V_1 \cdot \Delta T}}, \quad (13)$$

where A is a coefficient depending on the temperature stratification of the atmosphere, which determines the conditions for the horizontal and vertical dispersion of pollutants; M is the mass of pollutants emitted per unit time (i.e. the emission rate) (g/s); F is a dimensionless coefficient taking into account the deposition rate of pollutants (gaseous and aerosols, including solid particles) in the atmospheric air; m and n are dimen–sionless coefficients taking into account the conditions of emissions from the orifice of the pollution source; η is a dimensionless coefficient taking into account the influence of the terrain; H is the height of the emission source (m); V_1 is the pollutant flow rate (m^3/s); ΔT is the difference between the temperature of emitted pollutants T_p and the atmospheric air temperature T_a (°C).

Equation (12) cannot be used in the considered approach for several reasons:

- in our case, the source of pollutant emissions is area-based;
- the average speed of pollutants exiting the exhaust pipe when the vehicle is moving at above 0.5 m/s is assumed to be zero;
- pollutant temperature is close to the atmospheric air temperature;
- the vertical component of the pollutant speed is close to zero.

In this case, the following provision of the Order#804 [35] should be applied: "If the emission parameters of the source do not satisfy the conditions of the applicability of at least one emission calculation method (equation (12) in particular), during the calculations it is replaced by a virtual point or area source, which emission rate remains unchanged, the height H is taken equal to 2 m, the pollutant temperature T_p is set equal to the atmospheric air temperature T_a accepted in the calculation, and the average speed of pollutant exit from the orifice of the emission source is taken equal to zero". This provision confirms the validity of the proposed conceptual approach for considering multiple area sources of pollutant emissions at an intersection. In this case, we follow the provisions of [35] – which regulate the use of equation (13) for "cold emissions" – to calculate pollutant concentrations for emission sources, in which the vertical speed component of the gas-air mixture entering the atmosphere does not exceed 0.01 m/s, while the pressure, density, and temperature differ slightly from the relevant characteristics of atmospheric air:

$$C_m = \frac{A \cdot M \cdot F \cdot m' \cdot \eta}{H^{7/3}} \quad (14)$$

We use equation (14) to calculate the maximum ground level single concentration of pollutants C'_i from the i-th area source of unit used in final equation (10).

The maximum ground level concentration of pollutants C_m is achieved at a dangerous wind speed U_m at the distance X_m from the emission source. These accompanying reference parameters U_m and X_m are determined by several formulas in [35], which are not given here due to their bulkiness.

Step 2. Correction of calculations at an arbitrary wind speed U.

The maximum ground level concentration of pollu–tants $C_{m.U}$ under unfavorable meteorological conditions and a wind speed U different from the dangerous wind speed U_m is determined by the following scaling ratio:

$$C_{m.U} = r \cdot C_m, \quad (15)$$

where r is a dimensionless scaling factor determined by:

$$r = 0.67 \cdot \frac{U}{U_m} + 1.67 \cdot \left(\frac{U}{U_m}\right)^2 - \\ -1.34 \cdot \left(\frac{U}{U_m}\right)^3 \quad at \frac{U}{U_m} \leq 1; \quad (16)$$

$$r = \frac{3 \cdot U/U_m}{2 \cdot \left(U/U_m\right)^2 - U/U_m + 2} \quad at \frac{U}{U_m} > 1.$$

Fig. 3 graphically presents the dependence $r=f(U/U_m)$ as a correction for an arbitrary wind different from the reference value U_m.

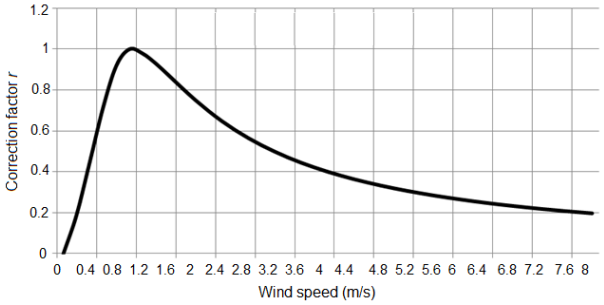

Figure 3. Correction factor *r* depending on an arbitrary wind speed *U*.

Fig. 3 shows that at a wind speed U different from the reference value U_m, the maximum calculated concentration C_m will always take lower values. The arbitrary wind speed U similarly affects the reference value X_m:

$$X_{m.U} = p \cdot X_m, \tag{17}$$

which is similarly expressed by the correction factor p with the relevant calculation formulas for the depen–dence $p=f(U/U_m)$:

$$\begin{aligned} p &= 3 \quad at \frac{U}{U_m} \le 0.25; \\ p &= 8.43 \cdot \left(1 - \frac{U}{U_m}\right)^5 + 1 \quad at \quad 0.25 < \frac{U}{U_m} \le 1; \\ p &= 0.32 \cdot \frac{U}{U_m} + 0.681 \quad at \frac{U}{U_m} > 1. \end{aligned} \tag{18}$$

Fig. 4 graphically presents the dependence $p= f(U/U_m)$ as a correction for an arbitrary wind speed different from the reference value Um. It shows that if the wind speed U differs from the reference value U_m, the dista-nce along the axis of the pollutant emission correspon-ding to the maximum emissions will always increase.

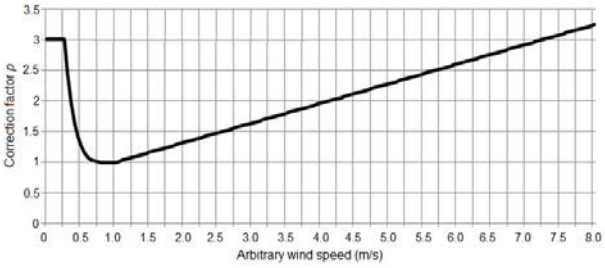

Figure 4. Correction factor *p* depending on an arbitrary wind speed *U*.

Step 3. Calculation of the pollutant concentration along the X emission axis

At the dangerous wind speed U_m, the ground level concentration C_x of pollutants in the atmospheric air from a point source on the emission axis, at various distances X from the emission source, is calculated similarly through a correction factor:

$$C_x = s_1 \cdot C_m, \tag{19}$$

where s_1 is a dimensionless coefficient determined depending on the X/X_m ratio using:

$$\begin{aligned} s_1 &= 3 \cdot \left(\frac{X}{X_m}\right)^4 - 8 \cdot \left(\frac{X}{X_m}\right)^3 + 6 \cdot \left(\frac{X}{X_m}\right)^2 \quad at \frac{X}{X_m} \le 1; \\ s_1 &= \frac{1.13}{0.13 \cdot \left(X/X_m\right)^2} \quad at 1 < \frac{X}{X_m} \le 8. \end{aligned} \tag{20}$$

Fig. 5 graphically presents the dependence $s_1= f(X/X_m)$ as a correction for the distance along the emission axis. It shows an almost exponential decrease in the concentration of pollutants when the actual distance differs from the reference value X_m.

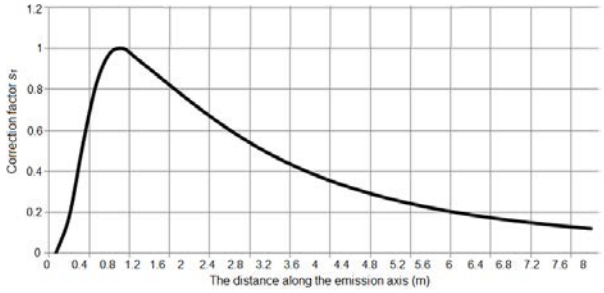

Figure 5. Correction factor s_1 depending on the distance along the emission axis

Step 4. Calculation of the pollutant concentration normal to the emission axis

The ground level concentration of pollutants in atmospheric air C_y is calculated similarly at the distance y normal to the emission axis through the scaling factor s_2 determined by:

$$C_y = s_2 \cdot C_x, \tag{21}$$

where s_2 is also a dimensionless coefficient:

$$\begin{aligned} s_2 &= \frac{1}{\left(1 + 5 \cdot t_y + 12.8y \cdot t_y^2 + 17 \cdot t_y^3 + 45.1 \cdot t_y^4\right)^2}, \\ &where \\ t_y &= \frac{U \cdot Y^2}{X^2} \quad at \quad U \le 5 \ (m/c) \\ t_y &= \frac{5 \cdot Y^2}{X^2} \quad at \quad U > 5 \ (m/c) \end{aligned} \tag{22}$$

Figure 6 shows the graphic dependence for $s_2= f(Y/X)$, which within $0<(Y/X)<0.5$ demonstrates a dec–rease in the concentration of emissions to almost zero with an almost Gaussian distribution.

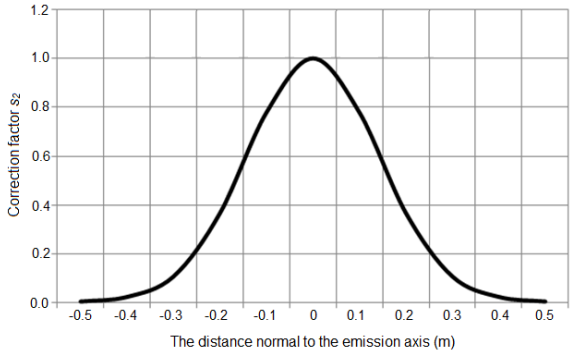

Figure 6. Correction factor s_2 depending on the distance normal to the emission axis.

The above equations allow the concentration of pollutant emissions to be calculated at an arbitrary point from an area source and, in the general form, to deter–mine the dispersion field of pollutant emissions from a single area source of a unit rate at a given wind speed.

The MatLab suite was used to carry out model experiments for determining the concentration field during the dispersion of pollutant emissions from an area source at a unit rate (in the individual case, at a wind speed U equal to the dangerous speed U_m).

The calculations used equations (18–21) with vari–ations in a distance X from the emission source and a distance Y normal to the emission axis.

Fig. 7 presents the modeling results in the form of a three-dimensional dispersion field of pollutant emis–sions from a source of a unit rate and at a wind speed U equal to the dangerous speed U_m.

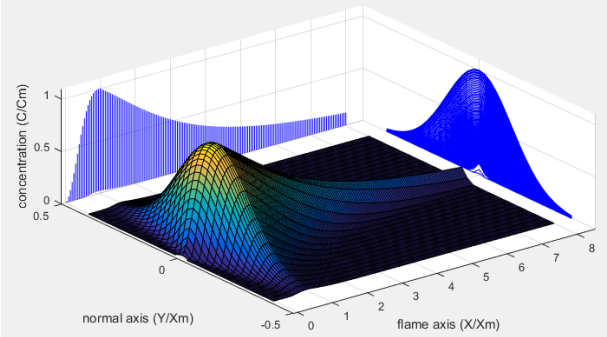

Figure 7. Pollution concentration field when emissions are dispersed from a source of a unit rate

The modeling results give a visualization of the real dispersion of emissions from a single (mobile) source, which is the basis for future estimates of the concentration fields of emissions from many randomly distributed single sources, both point and area.

5. A COMPLETE MATHEMATICAL MODEL FOR CALCULATING THE CONCENTRATION CLOUD FROM POLLUTANT EMISSIONS WITHIN THE ENTIRE INTERSECTION AREA

The final model represented by equation (10) is a mat–hematical macromodel for calculating the concentration of pollutants in any of the M squares of the dispersion cloud centered at point (x_m, y_m) from a set of N area sources of pollutant emissions centered at points (ξ_i, η_i), which make up the entire intersection. The calculation is carried out at a frequency of t_k, the minimum value of which is determined by the computing system.

The first term in this micromodel, M_i^{tk}, is the rate of the total pollutant emissions from the i-th area source determined by standing and moving vehicles in this area in time t_k. The mathematical model is represented by equation (12). The second term of this macromodel C'_i (x_m–ξ_i, y_m–η_i) is the partial concentration of pollutant emissions at point (x_m, y_m) from the i-th area source centered at point (ξ_i, η_i). It is determined through a set of correction factors for the maximum calculated concentration of pollutants (C_m in equation (14)) for the i-th area source (see Section 4).

The complete mathematical model of monitoring with a frequency of t_k at each point (x_m, y_m) of the pollutant concentration cloud C^{tk} (x_m, y_m) for an urban intersection divided into N area emission sources is represented by:

$$C^{t_k}(x_m, y_m) = \sum_{i=1}^{N} \left(M_i^{t_k} \cdot C'_i(x_m - \zeta_i, y_m - \eta_i) \right), \quad (23)$$

where

$$M_i^{t_k} = \frac{1}{60} \cdot \sum_{j=1}^{K_{si}} M_{sj} \cdot t_j^{idle} + \frac{1}{3600} \cdot \sum_{l=1}^{K_{mj}} r_{Vl} \cdot M_{ml} \cdot V_l \cdot t_{Vl},$$

$$C'_i\ (x_m - \zeta_i, y_m - \eta_i) =$$

$$= C_m \cdot r\left(\frac{U}{U_m}\right) \cdot s_1\left(\frac{X}{p \cdot X_m}\right) \cdot s_2\left(\frac{Y}{p \cdot X_m}\right)$$

6. THE DEVELOPMENT OF A SOFTWARE SYSTEM FOR CALCULATING POLLUTANT CONCENTRATIONS

The above mathematical model for the dynamic calcu–lation of a pollutant concentration cloud is implemented in Python programming language and added as a mo–dule into the AIMS eco software system. The sup–porting software solutions for this module are presented below.

The resulting detections from the YOLOv4 neural network for vehicles at an urban intersection are tracked in real time by the SORT tracker. Geographical coor–dinates are calculated for each vehicle and used as a basis for calculating the distance traveled, speed, idle time, and movement. All processed frames are stored in the memory and queued for processing. Each vehicle belongs to its own queue with unique data.

According to the regulatory documents, we calculate atmospheric emissions for the following pollutants emitted by a set of mobile sources:

- carbon monoxide CO;
- sum of nitrogen oxides (in terms of nitrogen dioxide) NOx;
- hydrocarbons;
- soot;
- sulfur dioxide SO2;
- formaldehyde CH2O;
- benz(a)pyrene C20H12;
- PM2.5;
- PM10.

Vehicle detections from the queue are used to calcu–late the amount of pollutant emissions with a frequency of 3 seconds. After the calculation, the queues are clea–red and refilled. An interval of 3 seconds was expe–rimentally selected as optimal for real-time operation. A shorter time interval leads to an increase in the number of processed video streams and the used software suite does not have enough time to calculate pollutant emis–sions and concentrations. Figure 8(a) shows detection queues over 3 seconds. Each point is a separate detec–tion. Separate tracers indicate a queue for one vehicle.

For the intersection area, all detections are divided into 20×20 meter cells, which corresponds to the area sources of pollutant emissions. The distance traveled, average speed, idle time, and movement time are calcu–

lated for each vehicle within each cell. Fig. 8(b) shows a fragment of a breakdown of detections into cells for the intersection area.

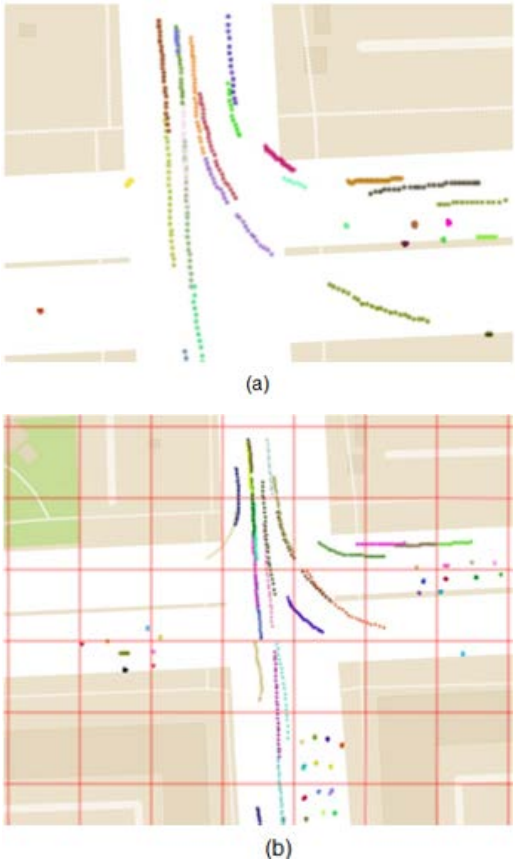

Figure 8. (a) Queues of vehicle detections with a frequency of 3 seconds; (b) Breakdown of detections into 20×20 meter cells

The cell size of 20×20 meters was chosen based on the optimal real-time operation of the computer system. A smaller size is insufficient to record vehicles moving at high speed. At a maximum speed of 60 km/h (16.7m/s), smaller cells will not have enough detections to calculate dynamic characteristics. For example, if a cell size is 10×10 meters and 8 frames are processed per second, only 4–5 detections will fall into the cell. This is not enough in view of the error of the neural network.

The total number of emissions is calculated based on all recorded detections within each cell. Thus, each cell represents an area emission source (Fig. 9). The amount of pollutants emitted into the atmospheric air per unit time (g/s) is calculated as the amount of emissions in grams divided by the time the vehicle is inside the cell.

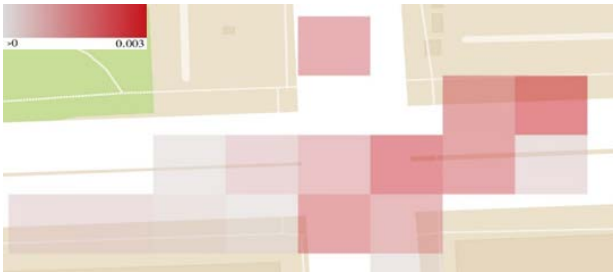

Figure 9. PM2.5 emissions in grams from area sources every 3 seconds

Taking into account the mathematical model equation (23), the following meteorological factors from the OpenWeather source are taken into account when calculating the concentrations of pollutants (mg/m^3) from traffic flow emissions in the ground level layer:

- ambient air temperature, ºC;
- wind speed, m/s;
- wind direction.

To calculate and display the pollutant cloud concen–tration for the entire intersection area, the area is divided into a 10×10 meter grid of squares. The concentration of emissions from each area source is calculated for each square of such a grid (Fig. 10).

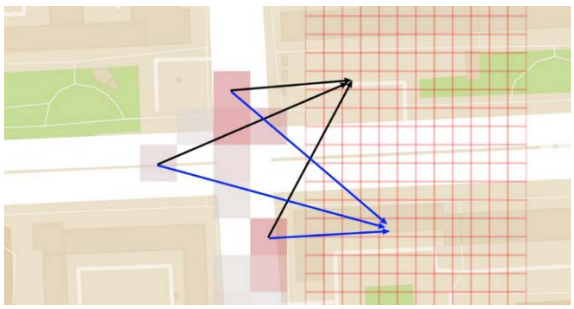

Figure 10. An example of summing emission concentra–tions from three area sources for two grid squares of the concentration cloud

The data are not taken into account immediately, but only after the time emissions from each area source need to reach all squares of the concentration cloud grid. To calculate the delay time, the distance between the source and the measurement area is divided by the wind speed. The result is stored in a list along with the time when the emissions reach the target. In each calculation iteration, all measurements from the list that have reached the square of the concentration cloud are added to the resulting concentration value.

Fig. 11 represents the shift in the concentration cloud of pollutant emissions under the influence of wind, generated by the new module of the AIMS eco software system for one intersection. The software system database generates a report on the quantity and concentrations of the main types of pollutants per day with a frequency of 20 minutes.

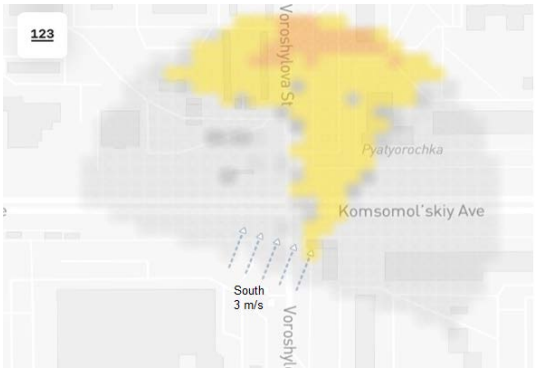

Figure 11. Time frame of monitoring the PM2.5 emission concentration cloud by the AIMS eco system

The depth of the reporting database in time is up to one year, which allows for further analytical studies of the environmental situation within the monitored intersections.

7. VERIFICATION OF THE METHODOLOGY FOR EMISSION CONCENTRATION MEASUREMENT

The results of modeling the concentrations of vehicle-related pollutant emissions were compared with instru–mental measurements made by a certified mobile laboratory in Magnitogorsk, with the wind at distances of 50m and 100m from the center of the intersection. C012M, AC32M, AF22M, G2107, DustTrak8533) la–boratory gas and dust analyzers and an WXT530 automatic weather station were used to measure pollutant concentrations.

Figs. 12–15 show the results of instrumental measu–rements averaged over 20 minutes and model calcu–lations every 2 minutes for the following pollutants: carbon monoxide CO; the sum of NOx (NO and NO2); and PM2.5 carried out over three days. Due to the influence of many unpredictable factors on instrumental measurements, verification comparison conditions pro–vided for the difference between the calculated values and the instrumental values by no more than 25% for one of three 20-minute intervals within one hour. This condition is met for all pollutants in the comparison tests

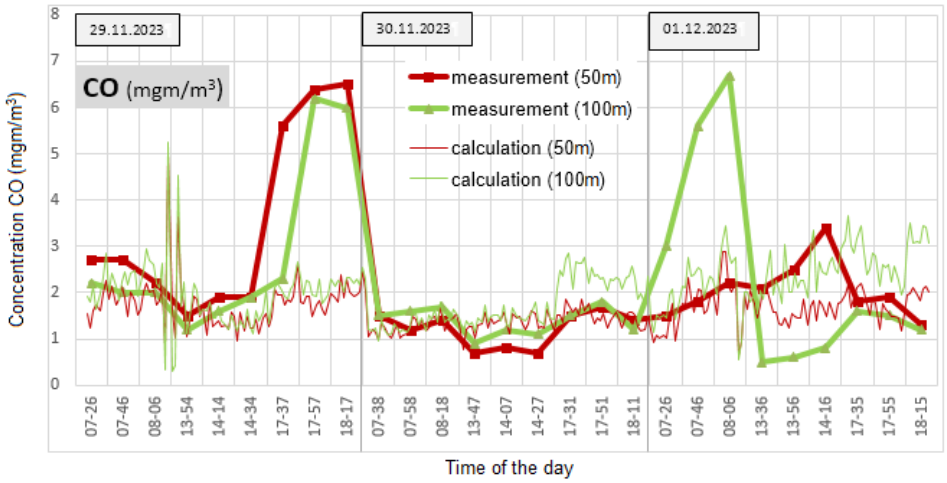

Figure 12. A comparison of CO emissions

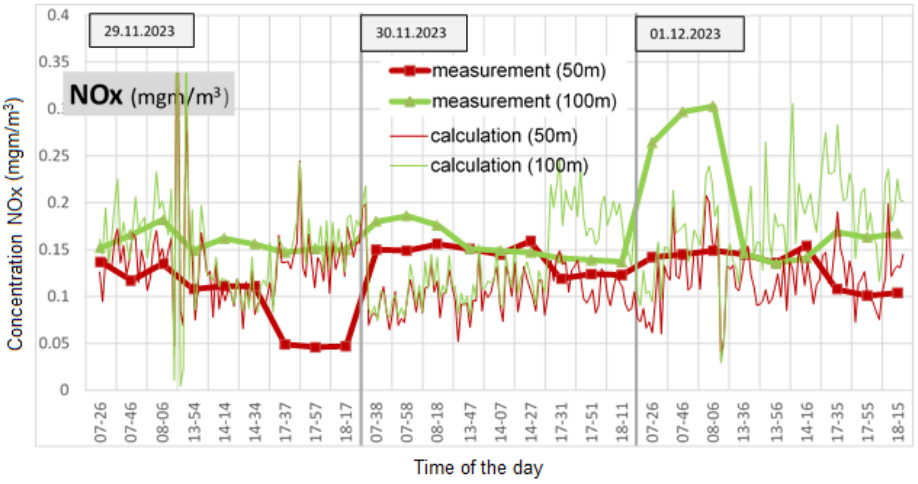

Figure 13. A comparison of NOx emissions

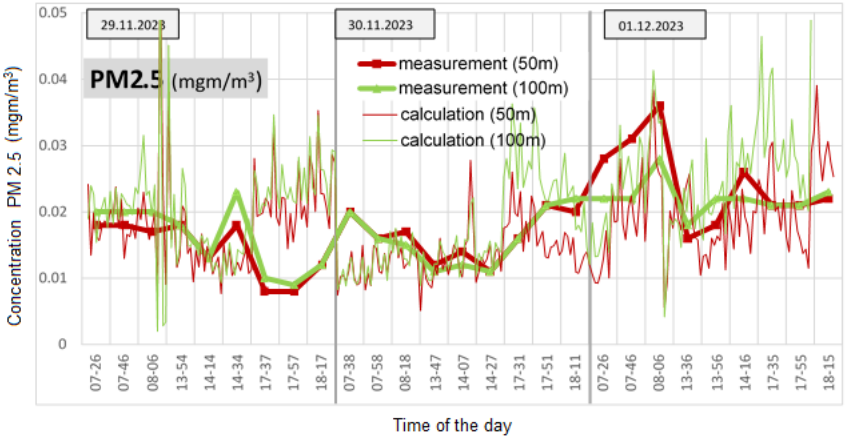

Figure 14. A comparison of PM2.5 emissions

When measuring PM2.5 emissions, the influence of random disturbances (end of the first day and beginning of the third day) is also manifested. In general, the average deviation of the calculated values of PM2.5 emissions is 8.7% for the measurement point 50m from the center of the intersection and 9.6% for the measurement point 100m from the center of the intersection (Fig. 14). The closeness of the calculated values of emissions obtained from modeling to the instrumental measurements shows the accuracy of the resulting mathematical model for the real-time assessment of the dispersion of vehicle-related emission concentrations.

8. CONCLUSIONS AND RECOMMENDATIONS FOR FUTURE WORK

In conclusion, we would like to emphasize the advantages of the developed approach to continuous monitoring of pollutant emissions based on the presented mathematical model. These advantages render our methodology more effective and relevant in the face of escalating environmental issues associated with motor vehicle traffic.

First and foremost, our solution provides real-time monitoring, which represents a significant advancement over traditional approaches. Most previous studies relied on static models that utilized historical data for computations. This limitation hindered timely responses to changes in traffic conditions. By collecting and analyzing data in real time, our model enables prompt detection and tracking of pollution levels, which is crucial for rapid response and implementation of measures to improve air quality.

Furthermore, we have integrated current meteorological conditions into the modeling process. By considering factors such as wind speed and direction, our approach offers improved conditions for predicting the dispersion of pollutants, thereby significantly enhancing the accuracy of our calculations. Many previous studies failed to account for the dynamic influence of meteorological conditions, often leading to outdated conclusions. In contrast, our methodology aims to provide a more comprehensive and realistic depiction of pollution distributions, which can have important implications for environmental policy and urban infrastructure.

The application of the YOLOv4 neural network for extracting and interpreting traffic flow data also represents a substantial improvement over traditional analysis methods. Our system demonstrates a high degree of adaptability and is capable of working with changing traffic patterns, whereas many prior studies depended on fixed parameters, overlooking the complex interactions within the system. This makes our model more flexible and viable in real-time conditions.

We also noted the high accuracy of our calculations, as demonstrated through comparative analysis with measurements obtained from a certified mobile laboratory. Our model showed deviations ranging from 5.9% to 13.4% for various pollutants, underscoring its reliability. Such a strong correlation with actual data indicates that our monitoring results can be trusted, thereby enhancing their practical significance.

An additional advantage of our approach is the capability to create dynamic maps of pollutant distributions at intersections. This fosters data visualization and makes the information accessible for analysis, which can become an important tool for environmental monitoring and strategic decision-making. In the context of existing static pollution maps, our method provides a more contemporary means of understanding the issue at the level of specific urban infrastructure segments.

In summary, although our model is currently simplified, there are clear pathways for its future development. We plan to integrate aspects related to urban development and account for the influence of surrounding buildings on wind flows and pollution distributions, which will offer even greater accuracy and reliability in our final calculations.

Thus, our research represents not only a vital step forward in the field of environmental air quality monitoring but also serves as a foundation for further advancements in urban air quality management, which is particularly pertinent in the context of contemporary environmental challenges. We hope that the findings of our study will be beneficial to both researchers and governmental agencies involved in the development of effective strategies for air quality improvement.

ACKNOWLEDGMENT

This research was supported by Russian Science Foundation, grant number 24-21-20086.

REFERENCES

[1] Khreis, H., Ramani, T., De Hoogh, K., Mueller, N., Rojas-Rueda, D., Zietsman, J., Nieuwenhuijsen, M. J.: Traffic-Related Air Pollution and the Local Burden of Childhood Asthma in Bradford, UK, International Journal of Transportation Science and Technology, Vol. 8, No. 2, pp. 116–128, 2019.

[2] Klems, J. P., Pennington, M. R., Zordan, C. A., McFadden, L., and Johnston, M. V.: Apportionment of Motor Vehicle Emissions from Fast Changes in Number Concentration and Chemical Composition of Ultrafine Particles Near a Roadway Intersection, Environmental Science & Technology, Vol. 45, No. 13, pp. 5637–5643, 2011.

[3] Song, J., Qiu, Z., Ren, G., and Li, X.: Prediction of Pedestrian Exposure to Traffic Particulate Matters (PMs) at Urban Signalized Intersection, Sustainable Cities and Society, Vol. 60, p. 102153, 2020.

[4] Jereb, B., Kumperščak, S., Bratina, T.: The Impact of Traffic Flow on Fuel Consumption Increase in the Urban Environment, FME Transaction, Vol. 46, No. 3, pp. 278–284, 2018.

[5] Jin, T., and Fu, L.: Application of GIS to Modified Models of Vehicle Emission Dispersion, Atmospheric Environment, Vol. 39, No. 34, pp. 6326–6333, 2005.

[6] Brunelli, U., La Pica, A., Pignato, L., Caminiti, D., Carollo, F.: Simulation with a Torque Dynamo–meter of Pollutants Emission from Vehicles Near Urban Cross-Road, in: *Proceedings of the Inter–national Body Engineering Conference & Exhibi–tion and Automotive & Transportation Technology Congress*, 9-11.07.2002 Paris, France.

[7] Sun, D. (Jian), Wu, S., Shen, S., and Xu, T.: Simulation and Assessment of Traffic Pollutant Dispersion at an Urban Signalized Intersection Using Multiple Platforms, Atmospheric Pollution Research, Vol. 12, No. 7, p. 101087, 2021.

[8] Zhu, S., Kim, I., Choi, K.: High-Resolution Simu–lation-Based Analysis of Leading Vehicle Accele–ration Profiles at Signalized Intersections for Emi–ssion Modeling, International Journal of Sustai–nable Transportation, Vol. 15, No. 5, pp. 375–385,2021.

[9] Hoydysh, W. G., and Dabberdt, W. F.: A Fluid Modeling Study of Concentration Distributions at Urban Intersections, Science of The Total Environ–ment, Vols. 146–147, pp. 425–432, 1994.

[10] Wang, Z., Lu, F., He, H., Lu, Q.-C., Wang, D., Peng, Z.-R.: Fine-Scale Estimation of Carbon Monoxide and Fine Particulate Matter Concentra–tions in Proximity to a Road Intersection by Using Wavelet Neural Network with Genetic Algorithm, Atmospheric Environment, Vol. 104, pp. 264–272, 2015.

[11] Söderena, P., Laurikko, J., Weber, C., Tilli, A., Kuikka, K., Kousa, A., Väkevä, O., Venho, A., Haaparanta, S., Nuottimäki, J.: Monitoring Euro 6 Diesel Passenger Cars NOx Emissions for One Year in Various Ambient Conditions with PEMS and NOx Sensors, Science of The Total Environ–ment, Vol. 746, p. 140971, 2020.

[12] Lei, J., Yang, C., Fu, Q., Chao, Y., Dai, J., and Yuan, Q.: An Approach of Localizing MOVES to Estimate Emission Factors of Trucks, International Journal of Transportation Science and Technology, p. S2046043023000059, 2023.

[13] Lyu, P., Wang, P. (Slade), Liu, Y., and Wang, Y.: Review of the Studies on Emission Evaluation Approaches for Operating Vehicles, Journal of Traffic and Transportation Engineering (English Edition), Vol. 8, No. 4, pp. 493–509, 2021.

[14] Jandacka, D., Decky, M., Durcanska, D.: Traffic Related Pollutants and Noise Emissions in the Vicinity of Different Types of Urban Crossroads, in: *Proceedings of the IOP Conference Series: Materials Science and Engineering*, 9–13.09.2019, Žilina, Slovakia, Vol. 661, No. 1, p. 012152.

[15] Li, W., Qiu, Z., and Wang, X.: Comparison of PM Spatiotemporal Variations and Exposure at Adjacent Signalized Intersection and Roundabout, Urban Climate, Vol. 50, p. 101590, 2023.

[16] Cerdeira, R., Louro, C., Coelho, L., Garcia, J., Gouveia, C., Coelho, P. J., and Bertrand, T.: Traffic Pollutant Emissions in Barreiro City, in: *Procee–dings of AIR POLLUTION 2007*, Algarve, Portugal, Vol. I, pp. 311–320, 2007.

[17] Sun, D. (Jian), Yin, Z., and Cao, P.: An Improved CAL3QHC Model and the Application in Vehicle Emission Mitigation Schemes for Urban Signalized Intersections, Building and Environment, Vol. 183p. 107213, 2020,.

[18] Jingguo, Q., Zheng, Z., Cui, Y., and Shi, L.: Study of Prediction of Motor Vehicles Emission Pollu–tants Concentration in Urban Street, International Journal of Digital Content Technology and its Applications, Vol. 6, pp. 9–16, 2012.

[19] Liu, J., Gao, Z., Wang, L., Li, Y., and Gao, C. Y.: The Impact of Urbanization on Wind Speed and Surface Aerodynamic Characteristics in Beijing during 1991–2011, Meteorology and Atmospheric Physics, Vol. 130, No. 3, pp. 311–324, 2018.

[20] Brzozowski, K., Ryguła, A., and Maczyński, A.: The Use of Low-Cost Sensors for Air Quality Ana–lysis in Road Intersections, Transportation Research Part D: Transport and Environment, Vol. 77, pp. 198–211, 2019.

[21] Oliveri Conti, G., Heibati, B., Kloog, I., Fiore, M., and Ferrante, M.: A Review of AirQ Models and Their Applications for Forecasting the Air Pollution Health Outcomes, Environmental Science and Pollution Research, Vol. 24, No. 7, pp. 6426–6445, 2017.

[22] Goel, A., Kumar, P.: A Review of Fundamental Drivers Governing the Emissions, Dispersion and Exposure to Vehicle-Emitted Nanoparticles at Sig–nalised Traffic Intersections, Atmospheric Environ–ment, Vol. 97, pp. 316–331, 2014.

[23] Chauhan, B. P., Joshi, G. J., Parida, P.: Car Fol–lowing Model for Urban Signalised Intersection to Estimate Speed Based Vehicle Exhaust Emissions, Urban Climate, Vol. 29, p. 100480, 2019.

[24] Pospisil, J., Jicha, M.: Numerical Modelling of Transient Dispersion of Air Pollution in Perpen–dicular Urban Street Intersection with Detail Inclu–sion of Traffic Dynamics, International Journal of Environment and Pollution, Vol. 65, No. 1/2/3, p. 71, 2019.

[25] Pepe, N., Pirovano, G., Balzarini, A., Toppetti, A., Riva, G. M., and Lonati, G.: Enhanced Air Quality Modelling through AUSTAL2000 Model in Milan Urban Area, in: *Proceedings of the IOP Conference Series: Earth and Environmental Science*, 4–5.09.2019, Milan, Italy,Vol. 296, No. 1, 2019, p. 012012.

[26] He, H., Lu, W.-Z., and Xue, Y.: Prediction of PM10 Concentrations at Urban Traffic Intersections Using Semi-Empirical Box Modelling with Instantaneous Velocity and Acceleration, Atmospheric Environ–ment, Vol. 43, No. 40, pp. 6336–6342, 2009.

[27] Sekar, C., Ojha, C. S. P., Gurjar, B. R., and Goyal, M. K.: Modeling and Prediction of Hourly Ambient Ozone (O3) and Oxides of Nitrogen (NOx) Con–centrations Using Artificial Neural Network and Decision Tree Algorithms for an Urban Intersection

in India, Journal of Hazardous, Toxic, and Radio–active Waste, Vol. 20, No. 4, p. A4015001, 2016.

[28] Fallah Shorshani, M., Franklin, M., Hatzopoulou, M.: Evaluation of Aggregate and Individual Vehi–cle Activity on Emissions Models and Their Impact on Air Quality, Atmospheric Pollution Research, Vol. 12, No. 5, p. 101052, 2021.

[29] Lejri, D. et al.: Acco–unting for Traffic Speed Dynamics When Calcu–lating COPERT and PHEM Pollutant Emissions at the Urban Scale, Transportation Research Part D: Transport and Environment, Vol. 63, pp. 588–603, 2018.

[30] Zheng, X., Yang, J.: CFD Simulations of Wind Flow and Pollutant Dispersion in a Street Canyon with Traffic Flow: Comparison between RANS and LES, Sustainable Cities and Society, Vol. 75, p. 103307, 2021.

[31] Ciric, I., Cojbasic, Z., Nikolic, V., Zivkovic, P., Tomic, M.: Air Quality Estimation by Computa–tional Intelligence Methodologies, Thermal Scie–nce, Vol. 16, No. suppl. 2, pp. 493–504, 2012.

[32] Agarwal, Y., Jain, K., Karabasoglu, O.: Smart Vehicle Monitoring and Assistance Using Cloud Computing in Vehicular Ad Hoc Networks, Inter–national Journal of Transportation Science and Technology, Vol. 7, No. 1, pp. 60–73, 2018.

[33] Lv, Z., Shang, W.: Impacts of Intelligent Trans–portation Systems on Energy Conservation and Emission Reduction of Transport Systems: A Com–prehensive Review, Green Technologies and Susta–inability, Vol. 1, No. 1, p. 100002, 2023.

[34] AIMS Eco. Real-time vehicle emissions monitoring system. https://aims.susu.ru/demo

[35] On Approval of Methods for Calculating the Dis–persion of Emissions of Harmful (Polluting) Subs–tances in the Atmospheric Air, Russian Federation, Jun 06 2017. https://docs.cntd.ru/document/45607 4826 (in Russian).

[36] DustTrak™ DRX Aerosol Monitor 8533 | TSI. https://tsi.com/products/aerosol-and-dust-monitors/ aerosol-and-dust-monitors/dusttrak%e2%84%a2-drx-aerosol-monitor-8533/

МОДЕЛ ДИНАМИЧКЕ НЕУРОНСКЕ МРЕЖЕ ЗА ПРАЋЕЊЕ ЖИВОТНЕ СРЕДИНЕ ЗАГАЂЕЊА ВОЗИЛА У УРБАНИМ УЛИЦАМА

В. Шепелев, А. Глушков, О. Иванова, К. Бастрикина

Загађење ваздуха гасовима емисијама возила у одрживом, паметном граду је неоспоран и хитан проблем који захтева нове методе решавања. Да би се предузеле административне мере за побољшање квалитета ваздуха, неопходно је имати поуздан алат за тренутну процену тренутног загађења ваздуха на раскрсницама путева као местима највећег гоми–лања возила. У овом чланку је описан математички модел и његова софтверска имплементација засно–вана на технологији неуронске мреже, која омо–гућава континуирано праћење емисија девет врста загађујућих материја из различитих категорија возила која стоје и крећу са параметрима као што су брзина, координате и време мировања. Аутори су развили скуп података за обуку динамичке неурон–ске мреже, који се састоји од 60.000 означених слика. Модел израчунава ниво загађења ваздушног базена на подручју одређеном зоном видљивости спољне камере за видео надзор и висином од 2 метра. За разлику од постојећих модела, предложено решење ради у режиму реалног времена, може се уградити у постојећу инфраструктуру за праћење раскрсница путева и узима у обзир тренутне вре–менске услове: јачину и смер ветра. Ово је омо–гућило ауторима да верификују резултате прорачуна инструменталним мерењима мобилне еколошке лабораторије, да постигну високу тачност у детек–цији тренутног загађења ваздуха за даље управљање еколошким ризицима повезаним са друмским саобраћајем.